

Molecular Mechanisms of Calmodulin Action on TRPV5 and Modulation by Parathyroid Hormone^{∇†}

Theun de Groot,^{1‡} Nadezda V. Kovalevskaya,^{2‡} Sjoerd Verkaart,¹ Nathalie Schilderink,² Marco Felici,² Eline A. E. van der Hagen,¹ René J. M. Bindels,¹ Geerten W. Vuister,² and Joost G. Hoenderop^{1*}

Department of Physiology, Nijmegen Center for Molecular Life Sciences, Radboud University Nijmegen Medical Center, Netherlands,¹ and Department of Protein Biophysics, Institute of Molecules and Materials, Radboud University Nijmegen, Netherlands²

Received 18 November 2010/Returned for modification 7 February 2011/Accepted 29 April 2011

The epithelial Ca²⁺ channel transient receptor potential vanilloid 5 (TRPV5) constitutes the apical entry gate for active Ca²⁺ reabsorption in the kidney. Ca²⁺ influx through TRPV5 induces rapid channel inactivation, preventing excessive Ca²⁺ influx. This inactivation is mediated by the last ~30 residues of the carboxy (C) terminus of the channel. Since the Ca²⁺-sensing protein calmodulin has been implicated in Ca²⁺-dependent regulation of several TRP channels, the potential role of calmodulin in TRPV5 function was investigated. High-resolution nuclear magnetic resonance (NMR) spectroscopy revealed a Ca²⁺-dependent interaction between calmodulin and a C-terminal fragment of TRPV5 (residues 696 to 729) in which one calmodulin binds two TRPV5 C termini. The TRPV5 residues involved in calmodulin binding were mutated to study the functional consequence of releasing calmodulin from the C terminus. The point mutants TRPV5-W702A and TRPV5-R706E, lacking calmodulin binding, displayed a strongly diminished Ca²⁺-dependent inactivation compared to wild-type TRPV5, as demonstrated by patch clamp analysis. Finally, parathyroid hormone (PTH) induced protein kinase A (PKA)-dependent phosphorylation of residue T709, which diminished calmodulin binding to TRPV5 and thereby enhanced channel open probability. The TRPV5-W702A mutant exhibited a significantly increased channel open probability and was not further stimulated by PTH. Thus, calmodulin negatively modulates TRPV5 activity, which is reversed by PTH-mediated channel phosphorylation.

TRPV5 belongs to the transient receptor potential (TRP) superfamily of cation-selective ion channels with comparable molecular architecture but versatile physiological functions (20). Based on the homology, TRP channels are classified within six related subfamilies: classical or canonical (TRPC), melastatin-related (TRPM), polycystins (TRPP), mucolipins (TRPML), ANKTM1-related (TRPA), and vanilloid receptor-related (TRPV). Of all TRP channels, TRPV6 holds the highest homology with TRPV5 (30). Both are highly Ca²⁺ selective and share biophysical properties clearly distinct from other TRP channels. Generation of TRPV5 knockout mice demonstrated the critical role of TRPV5 as gatekeeper of active Ca²⁺ reabsorption in the renal handling of Ca²⁺ (13).

TRPV5 contains six putative transmembrane domains and intracellular amino (N) and C termini. A functional TRPV5 channel exists as a tetramer comprising a central Ca²⁺-selective pore by the hydrophobic region between transmembrane domains 5 and 6 (30). Electrophysiological studies of human embryonic kidney 293 (HEK293) cells heterologously expressing TRPV5 demonstrated that the channel is constitutively active at physiological membrane potentials as no stimulus or ligand was required for TRPV5-mediated Ca²⁺ entry (12, 32).

The Ca²⁺ current amplitude of TRPV5 is highly dependent on the electrochemical gradient. Increasing extracellular Ca²⁺ levels or the negative membrane potential amplified the Ca²⁺ current, resulting in an elevated intracellular Ca²⁺ concentration ([Ca²⁺]_i) (32). In the absence of Ca²⁺ ions, TRPV5 is also permeable to monovalent cations (32). The residue D542 of TRPV5 is essential for Ca²⁺ selectivity and permeability (22, 24). Alanine substitution at this position yielded a mutant channel (D542A) in which Ca²⁺ permeation was blocked while it was still permeable for Na⁺ (24).

To prevent excessive Ca²⁺ influx, TRPV5 harbors a Ca²⁺-dependent feedback mechanism allowing rapid inactivation of the channel. The rate of TRPV5 inactivation correlated directly with the Ca²⁺ current amplitude, indicating that the influx of Ca²⁺ inhibits channel activity (23, 32, 33). Moreover, this inhibition was absent when Na⁺ was used as the charge carrier (32). Besides the influx of Ca²⁺ through the pore, the channel was also shown to be sensitive to resting intracellular Ca²⁺ concentrations (22). Increasing levels of intracellular Ca²⁺ lowered TRPV5-mediated Na⁺ currents in a concentration-dependent manner (22). Convincingly, these effects were also observed for the Ca²⁺-impermeable D542A mutant (22). Therefore, it was suggested that Ca²⁺ entry through TRPV5 elevates the local Ca²⁺ concentration in a microdomain near the channel pore, resulting in channel inactivation (22).

In 2003, Nilius et al. demonstrated that the C terminus of TRPV5 plays a role in Ca²⁺-induced inactivation (25). Removal of the last 30 amino acids rendered the channel less sensitive for Ca²⁺ (25). Until now, the molecular mechanism for Ca²⁺-dependent inactivation of TRPV5 has remained elusive. For TRPV6, a close homologue of TRPV5, it was shown

* Corresponding author. Mailing address: Nijmegen Center for Molecular Life Sciences, 286 Physiology, Radboud University Nijmegen Medical Center, P.O. Box 9101, 6500 HB Nijmegen, Netherlands. Phone: 31 24 3610580. Fax: 31 24 3616413. E-mail: j.hoenderop@fysiol.umcn.nl.

‡ T.D.G. and N.V.K. contributed equally to this work.

† Supplemental material for this article may be found at <http://mcb.asm.org/>.

∇ Published ahead of print on 16 May 2011.

that Ca^{2+} -dependent inactivation is regulated by the Ca^{2+} -sensing protein calmodulin via binding to the channel's C terminus (residues 691 to 711) (16, 21). Calmodulin inhibited TRPV6 activity, which was counteracted by protein kinase C-mediated phosphorylation of the T702 residue (21). Although calmodulin did bind to the TRPV5 C terminus (16), no role for this binding in the channel regulation was identified. Interestingly, calmodulin also binds and regulates many other TRP channels although the precise role of calmodulin in channel functioning remains to be identified (37).

The aim of the present study was to unravel the molecular mechanism underlying Ca^{2+} -dependent TRPV5 inactivation. Therefore, we combined functional methods such as fura-2 measurements and patch clamp analysis with nuclear magnetic resonance (NMR) spectroscopy, a technique providing information about molecular interactions at the atomic level.

MATERIALS AND METHODS

Protein expression and purification. For production of the uniformly ^{13}C - and/or ^{15}N -labeled C-terminal calmodulin binding domain of human TRPV5 (residues 696 to 729 [hTRPV5⁶⁹⁶⁻⁷²⁹]), a recombinant approach was used. A synthetic gene optimized for *Escherichia coli* was purchased from Mr. Gene GmbH (Regensburg, Germany). The coding sequence was cloned into a pGEV2 expression vector (14). The fusion protein with an N-terminal GB1 tag and C-terminal His₆ tag was overexpressed in M9 minimal medium containing 4 g/liter [$^{13}\text{C}_6$]glucose and/or 1 g/liter [^{15}N]ammonium chloride (Buchem BV, Apeldoorn, Netherlands) as the sole source of carbon and/or nitrogen, respectively. The GB1-hTRPV5⁶⁹⁶⁻⁷²⁹-His₆ fusion protein was purified by affinity chromatography using IgG-Sepharose (GE Healthcare) according to the manufacturer's instructions. The final purification step was done via ion-exchange chromatography using a MonoQ 5/50 column (GE Healthcare). The GB1 tag was cut by thrombin (Sigma-Aldrich) according to the manufacturer's instructions. hTRPV5⁶⁹⁶⁻⁷²⁹ with a C-terminal His₆ tag was further purified by IgG-Sepharose.

Nonlabeled and uniformly ^{15}N -labeled recombinant *Xenopus laevis* calmodulin (identical to mammalian) was expressed in *E. coli* AR58 cells carrying the pTncoI2 plasmid (kind gift of C. Klee, NIH, Bethesda, MD). Expression was induced by a temperature shift from 30°C to 42°C, and 3 to 4 h after induction cells were harvested and lysed. Calmodulin was purified by weak anion exchange (DEAE; GE Life Sciences) and affinity chromatography (Phenylsepharose; GE Life Sciences). Purified protein was dialyzed against a 1/100 mixture of 50 mM KCl, 10 mM CaCl_2 , and 20 mM Tris (pH 7.0)-HCl buffer, freeze-dried, and stored at -20°C.

Peptide synthesis. Peptide hTRPV5⁶⁹⁶⁻⁷²⁹ (GSHRGWEILRQNTLGHNLGLNLSEGDGEEVYHF) corresponding to residues 696 to 729 of hTRPV5 (with an N-terminal Ser mutated to Gly) was purchased from Peptides and Elephants GmbH (Potsdam, Germany). It was purified by high-performance liquid chromatography ([HPLC] >95% purity) and analyzed by mass spectrometry.

NMR sample preparation. For the NMR titration of ^{15}N -labeled calmodulin by synthetic peptide hTRPV5⁶⁹⁶⁻⁷²⁹, a series of samples with a protein-ligand molar ratio ranging from 1:0 to 1:4 was prepared. Due to solubility problems, the peptide was first dissolved in 20 mM Tris (pH 8.5)-HCl, mixed with calmodulin in an appropriate ratio, and then dialyzed against a 1/100 mixture of 50 mM KCl, 10 mM CaCl_2 , and 20 mM Tris (pH 7.0)-HCl. After lyophilization the samples were reconstituted in 50 mM KCl, 10 mM CaCl_2 , and 20 mM Tris (pH 7.0)-HCl. D_2O and NaN_3 (both from Sigma-Aldrich) were added to the NMR samples to final concentrations of 5 to 7% (vol/vol) and 0.01% (vol/vol), respectively. The concentration of calmodulin in the samples was ~200 μM . Due to already mentioned solubility problems, ^{13}C - and/or ^{15}N -labeled hTRPV5⁶⁹⁶⁻⁷²⁹-His₆ was dissolved in 10 mM CaCl_2 -10 mM $\text{CH}_3\text{COONH}_4$ (pH 5.0)-NaOH. For titration, the nonlabeled calmodulin was dissolved in the same buffer. The concentration of ^{13}C , ^{15}N -labeled hTRPV5⁶⁹⁶⁻⁷²⁹-His₆ was ~150 μM .

NMR spectroscopy. Spectra were recorded at 298 K on a Varian Inova 600 or 800 MHz equipped with a standard triple resonance probe and a cold probe, respectively. For titration of calmodulin with peptide (and vice versa), two-dimensional (2D) ^{15}N - ^1H -heteronuclear single-quantum coherence (HSQC) spectra were recorded. For sequential assignment of hTRPV5⁶⁹⁶⁻⁷²⁹, three-dimensional (3D) HNCACB and CBCA(CO)NH experiments were performed.

All spectra were processed by NMRpipe suite (7) and analyzed by the program CcpNmr Analysis (34).

Construction of mammalian expression vectors. The human parathyroid hormone (hPTH) receptor cDNA was cloned in the pCB7 vector behind a phosphoglycerate kinase (PGK) promoter using HindIII and BamHI. The bicistronic expression vector pCINeo/IRES-eGFP (where IRES is internal ribosome entry site) was implemented for coexpression of rabbit TRPV5 containing an N-terminally fused hemagglutinin (HA) tag and enhanced green fluorescent protein (eGFP). The rabbit TRPV5 C terminus (amino acids 617 to 730) was cloned into the pGEX 6p-2 vector. Mutations in TRPV5 and glutathione S transferase (GST)-TRPV5 were introduced using site-directed mutagenesis (Stratagene, La Jolla, CA), according to the manufacturer's protocol, after which all plasmids were sequence verified.

Cell culture and transfection. HEK293 cells were grown in Dulbecco's modified Eagle's medium (DMEM; Bio Whittaker Europe, Vervier, Belgium) containing 10% (vol/vol) fetal calf serum (PAA, Linz, Austria), 2 mM L-glutamine, and 10 μM /ml nonessential amino acids at 37°C in a humidity-controlled incubator with 5% (vol/vol) CO_2 . Cells were transiently transfected with the appropriate plasmids using polyethylenimine (PEI; Brunswig/PolySciences Inc.) with a DNA-PEI ratio of 6:1 for biochemical or live-cell imaging experiments. For patch clamp experiments, cells were transiently transfected with the appropriate plasmids using Lipofectamine 2000 (Invitrogen, Breda, Netherlands). For all experiments, transfected cells were used after 24 h.

Calmodulin precipitation assay. Calmodulin-coupled Sepharose 4B beads (GE Healthcare Bio-Sciences AB, Uppsala, Sweden) were incubated for 60 min at room temperature (RT) with bacterial lysate containing GST, GST fused to the wild-type TRPV5 (GST-TRPV5-WT), and point mutants, as previously described (31). After extensive washing using Tris-buffered saline (pH 7.4) containing 2% (vol/vol) Triton X-100 and protease inhibitors, proteins were eluted from beads with SDS-PAGE loading buffer, separated on an SDS-polyacrylamide gel, and analyzed by immunoblotting using an anti-GST antibody (1:2,000; Sigma-Aldrich, St. Louis, MO).

Intracellular Ca^{2+} measurements using fura-2-AM. HEK293 cells were seeded on fibronectin-coated coverslips (diameter, 25 mm) and transfected with the appropriate pCINeo/IRES-eGFP vector. After 24 h, cells were loaded with 3 μM fura-2-acetoxymethyl ester (fura-2-AM; Molecular Probes) and 0.01% (vol/vol) Pluronic F-129 (Molecular Probes) in DMEM at 37°C for 20 min. After cells were loaded, they were washed twice with phosphate-buffered saline (PBS) and allowed to equilibrate at 37°C for another 10 min in 132.0 mM NaCl, 4.2 mM KCl, 1.4 mM CaCl_2 , 1.0 mM MgCl_2 , 5.5 mM D-glucose, and 10 mM HEPES (pH 7.4)-Tris. For Ca^{2+} -free conditions, a similar buffer composition was used in which Ca^{2+} was replaced with 2 mM EGTA.

Details of microscopy procedures and quantitative image analysis have been described previously (6). In short, fura-2-loaded cells were placed on an inverted microscope using an incubation chamber. Changes in extracellular Ca^{2+} were facilitated using a perfusion system, and the resulting changes in Ca^{2+} were monitored with fura-2 excited at 340 and 380 nm. Only those cells responding to a Ca^{2+} -EGTA- Ca^{2+} treatment were included. All measurements were performed at room temperature. Full-length human PTH (Bachem AG, Bubendorf, Switzerland) was added at 75 s after the start of recording.

Electrophysiology. Patch clamp experiments were performed as described previously (24, 32) in the tight-seal whole-cell configuration at room temperature using an EPC-10 patch clamp amplifier controlled by the Pulse software (HEKA Elektronik, Lambrecht, Germany). Cells were kept in nominal divalent-free solution to prevent Ca^{2+} overload. For whole-cell patch clamp, patch pipettes had a resistance between 2 and 4 M Ω after they were filled with the standard intracellular solution (5). Cells were held at +20 mV, and voltage ramps of 450 ms ranging from -100 to +100 mV were applied to measure current/voltage (*I/V*) relations. Ca^{2+} currents were measured for 3 s at -100 mV stepping from a holding potential of +70 mV. Cell capacitance and access resistance were continuously monitored using the automatic capacitance compensation of the Pulse software. Current densities were obtained by normalizing the current amplitude to the cell membrane capacitance. Whole-cell patch clamp data were analyzed using Igor Pro software (WaveMetrics, Lake Oswego, OR). For cell-attached single-channel recordings, pipette resistance was between 7 and 10 M Ω . Cells were perfused with the following solution: 140 mM KCl, 5 mM EDTA, 5 mM EGTA, 1 mM MgCl_2 , 10 mM glucose, and 10 mM HEPES (pH 7.2)-KOH. The pipette contained 140 mM NaCl, 10 mM EGTA, and 10 mM HEPES (pH 7.2)-NaOH. The sampling rate was 10 kHz; currents were filtered at 1 kHz. The analysis of single-channel data was performed using TAC software (Bruyton, Seattle, WA). Channel conductance was measured using a step protocol ranging from -100 mV to +80 mV in 20-mV increments, and every step lasted for 2 s.

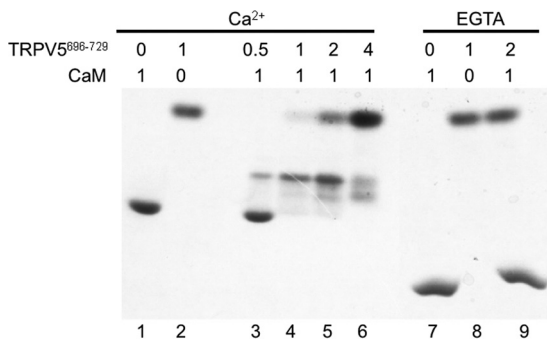


FIG. 1. Calmodulin binding to the TRPV5 C terminus. A native polyacrylamide gel, demonstrating interactions between calmodulin (CaM) and hTRPV5⁶⁹⁶⁻⁷²⁹, is shown. Lanes 1 and 7 contain calmodulin in the presence of Ca²⁺ and EGTA, respectively; lanes 2 and 8 contain hTRPV5⁶⁹⁶⁻⁷²⁹ in the presence of Ca²⁺ and EGTA, respectively. The gel demonstrates that in the presence of calcium, calmodulin is forming complexes with hTRPV5⁶⁹⁶⁻⁷²⁹ (lanes 3 to 6 contain calmodulin and hTRPV5⁶⁹⁶⁻⁷²⁹ at different ratios in the presence of Ca²⁺). In the presence of EGTA, no interactions are detected. It should be noted that the proteins in the absence of SDS separate on the basis of their charge-to-mass ratios. Proteins with higher molecular weight may, in fact, run faster than those with the lower molecular weight.

Statistical analysis. Numerical results were visualized using Origin Pro, version 7.5 (OriginLab Corp., Northampton, MA), and are presented as the mean \pm standard error of the mean (SEM). Statistical differences were determined using a one-way analysis of variance (ANOVA), followed by a Newman-Keuls multiple comparison test. *P* values below 0.05 were considered significant.

RESULTS

The C terminus of TRPV5 binds calmodulin in a Ca²⁺-dependent manner. To study the role of the last 30 amino acids of TRPV5 in relation to the Ca²⁺-induced channel inactivation (9), we investigated this C-terminal part of TRPV5 for potential calmodulin binding. Native polyacrylamide gel electrophoresis was used to study *in vitro* interactions of calmodulin with the synthetic peptide hTRPV5⁶⁹⁶⁻⁷²⁹. Lanes 1 and 2 of Fig. 1 depict calmodulin and hTRPV5⁶⁹⁶⁻⁷²⁹ peptide, respectively, in the presence of Ca²⁺. Combining calmodulin and hTRPV5⁶⁹⁶⁻⁷²⁹ at a 1:0.5 molar ratio in the presence of Ca²⁺ (lane 3) eliminated the band previously visible at the height of the free peptide. This suggests that the TRPV5 peptide is bound by calmodulin, and this calmodulin-hTRPV5⁶⁹⁶⁻⁷²⁹ complex appeared as a band above free calmodulin. Upon increase of the peptide concentration (Fig. 1, lanes 4 to 6), the band of free calmodulin disappeared, and the formation of a second complex was detected. In the presence of EGTA (lanes 7 to 9), calmodulin migrated to a lower height within the gel, and complex formation of calmodulin-hTRPV5⁶⁹⁶⁻⁷²⁹ was not detected.

Specific binding of hTRPV5⁶⁹⁶⁻⁷²⁹ to calmodulin is confirmed by NMR spectroscopy. Chemical shift perturbation (CSP) experiments are widely used to define binding sites in biomolecular complexes. In particular, 2D heteronuclear single quantum coherence (HSQC) experiments are often used in protein NMR spectroscopy to study *in vitro* interactions (3). The resulting two-dimensional spectrum contains chemical shifts of ¹H on one axis and chemical shifts of a directly attached het-

eronucleus (i.e., ¹⁵N for ¹⁵N-¹H-HSQC) on the second axis, and each peak corresponds to a unique amide proton. For example, in an HSQC spectrum of ¹⁵N-labeled protein, when an interaction of the protein under consideration with another molecule occurs, the peaks corresponding to specific amino acids involved in this interaction will change their position in the spectrum (chemical shift perturbation) and thus will allow the determination of the binding site. It should be noted that CSPs not only may arise from direct interaction with a binding partner but also may be caused by allosteric effects and structural changes in the protein upon binding. Thus, the residues with the largest CSPs are suggested to be located at only critical spots in the binding interface. ¹⁵N-¹H-HSQC spectra of free ¹⁵N-labeled hTRPV5⁶⁹⁶⁻⁷²⁹ and hTRPV5⁶⁹⁶⁻⁷²⁹ in the presence of calmodulin are shown in Fig. 2A.

Sequential assignment (defining which peak corresponds to which amino acid) was performed using 3D HNCACB and CBCA(CO)NH spectra. For the free hTRPV5⁶⁹⁶⁻⁷²⁹ peptide, it was possible to unambiguously assign HN, N, H α , C α , and C β for \sim 80% of the residues (deposited in the Biological Magnetic Resonance Bank [BMRB], entry 17472). Free peptides of \sim 35 amino acids are often unstructured, as demonstrated by the narrow dispersion of the hTRPV5⁶⁹⁶⁻⁷²⁹ backbone amide resonances: most of the peaks are located in the region of the spectrum characteristic for random coil proteins (¹H chemical shift of 7.6 to 8.2 ppm). Likewise, secondary structure prediction based on chemical shifts of C α , C β , and H α confirmed the absence of distinct structured elements in free hTRPV5⁶⁹⁶⁻⁷²⁹ (data not shown). Addition of nonlabeled calmodulin to the ¹⁵N-labeled free peptide leads to the changes in ¹⁵N-¹H-HSQC spectrum, indicating a binding event (Fig. 2A). A visible increase in spectral dispersion of amide resonances upon addition of calmodulin (red spectrum) indicated conformational changes in the peptide. Peaks unambiguously assigned to the residues of the putative calmodulin binding site (R699, W701, L704, R705, T708, and L709) were shifted in the ¹⁵N-¹H-HSQC spectrum of hTRPV5⁶⁹⁶⁻⁷²⁹ in the presence of calmodulin, which demonstrated their direct role in the binding. Convincingly, the side chain of W701 also interacted with calmodulin since a very large ¹H chemical shift difference (>0.6 ppm) was observed for the amino group of the W701 indol ring between bound and nonbound forms. Similarly, the peaks corresponding to Ne of R699 and R705 were almost absent in the free peptide but were clearly visible and shifted in the presence of calmodulin (¹H chemical shift difference of up to 0.25 ppm; ¹⁵N chemical shift difference of >2 ppm). This fact strongly suggested that the guanidinium groups of R699 and R705 are also involved in the interaction.

Stoichiometry of binding: one calmodulin per two hTRPV5⁶⁹⁶⁻⁷²⁹ peptides. Titration of ¹⁵N-labeled calmodulin by nonlabeled synthetic peptide hTRPV5⁶⁹⁶⁻⁷²⁹ reflected the changes in calmodulin upon peptide binding. Three ¹⁵N-¹H-HSQC spectra of the complexes with calmodulin-hTRPV5⁶⁹⁶⁻⁷²⁹ at molar ratios of 1:0 (black), 1:1 (red), and 1:2 (blue) were recorded and are displayed superimposed in Fig. 2B. By partial assignment of calmodulin (for well-resolved resonances) using previously published results (2), it was determined that the resonances belonging to the residues of both the N and C domains of calmodulin (residues 1 to 79 and 81 to 148, respectively) were significantly shifted

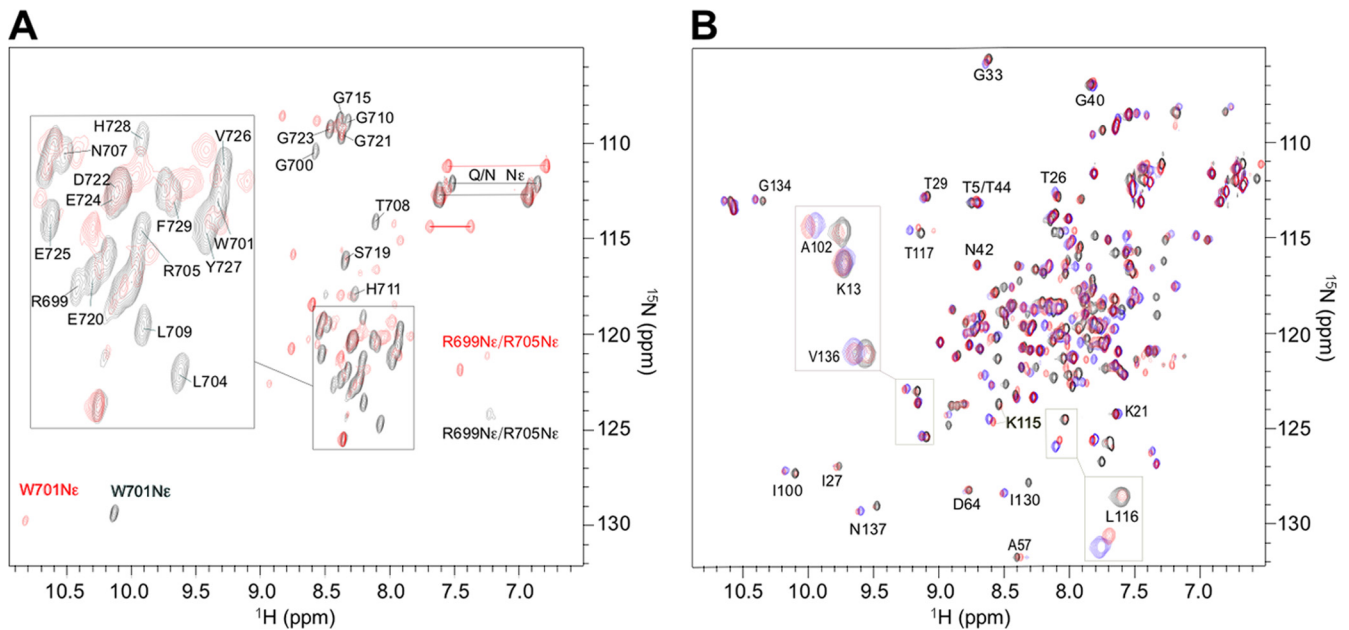


FIG. 2. *In vitro* binding of hTRPV5^{696–729} to calmodulin. (A) ^{15}N - ^1H -HSQC spectra of hTRPV5^{696–729} in the absence of calmodulin (black) and in the presence of 4-fold excess of calmodulin (red). Each peak corresponds to a unique proton attached to a ^{15}N nucleus. Amino acid residues are marked for which assignment is unambiguous. Ne, nitrogen atom of the side chain amide group R, W, and Q/N. (B) ^{15}N - ^1H -HSQC spectra of calmodulin at various concentrations of the synthetic peptide hTRPV5^{696–729}. Calmodulin-peptide molar ratios are represented as follows: black, 1:0; red, 1:1 complex; blue, 1:2 complex.

in the presence of hTRPV5^{696–729}. Remarkably, in the ^{15}N - ^1H -HSQC spectra at 1:1 molar ratio (Fig. 2B, red), several residues display two peaks, e.g., A102, K115, and L116. One peak is related to the free Ca^{2+} /calmodulin as it is situated very close to or directly at the position of the free Ca^{2+} /calmodulin; the other peak corresponds to the peptide-bound calmodulin. Upon increasing hTRPV5^{696–729} concentration to a calmodulin/hTRPV5^{696–729} molar ratio of 1:2 (Fig. 2B, blue spectrum), all double peaks collapsed into single peaks, and most of these did not coincide with the bound form at a 1:1 molar ratio, which implied the presence of a second binding event. Upon further addition of hTRPV5^{696–729}, only minor changes were detected that included shifting of the equilibrium toward a 1:2 complex and sharpening of the resonances (data not shown).

Mutation of the TRPV5 C terminus reduces calmodulin binding. To investigate the role of calmodulin in channel function, the residues suggested by the NMR spectroscopy to be crucial for calmodulin binding were mutated. First, the binding to calmodulin was assessed. Calmodulin immobilized on Sepharose beads was implemented to precipitate the glutathione *S*-transferase (GST)-tagged TRPV5 C terminus (residues 617 to 730). The mutation analysis and subsequent functional studies were performed with the rabbit isoform of TRPV5 as this isoform is generally used by our laboratory to study TRPV5 function. The rabbit and human C termini are highly conserved (Fig. 3A). First, GST-TRPV5 precipitation was studied in the presence of EGTA or Ca^{2+} and compared to the results with GST alone. The calmodulin beads precipitated GST-TRPV5 in the presence of Ca^{2+} while both GST alone and TRPV5 in the absence of Ca^{2+} (EGTA) were not precipitated by calmodulin (Fig. 3B and C). Second, the positively charged residues with the largest CSPs were replaced by negatively charged residues,

resulting in the point mutants TRPV5-H699D, -R700E, -R706E, and -R707E. Substitution of the positive charges significantly reduced TRPV5 precipitation by calmodulin (Fig. 3D and E). Mutation of residue R690, which is outside the proposed calmodulin binding region, did not affect TRPV5 binding to calmodulin (Fig. 3D and E). Third, the bulky hydrophobic residues with large CSPs were replaced by the small hydrophobic residue alanine. These mutants, W702A, L705A, and L710A, exhibited a significantly reduced precipitation by calmodulin compared to precipitation of wild-type TRPV5 (TRPV5-WT) protein (Fig. 3F and G).

Calmodulin binding determines TRPV5 activity. Next, the effect of the various point mutations on TRPV5 function was studied. Therefore, the point mutations described above were introduced in the full-length TRPV5 protein, which was subsequently expressed in HEK293 cells. The $[\text{Ca}^{2+}]_i$ was assessed by fura-2 analysis as a measurement for TRPV5 activity (6). Figure 4A and B show typical fura-2 traces of the various mutated TRPV5 proteins over time. Statistical analysis of $[\text{Ca}^{2+}]_i$ at time (*t*) zero (0 min; basal conditions) demonstrated that all point mutations presumed to be located within the calmodulin binding domain caused an elevation of $[\text{Ca}^{2+}]_i$ compared to the WT channel level (Fig. 4C). The W702A and R706E mutants, displaying virtually complete loss of calmodulin binding, exhibited the highest $[\text{Ca}^{2+}]_i$ of all mutants (Fig. 4C). The R690E mutation, which falls outside the calmodulin binding domain and, therefore, had no effect on calmodulin interaction, did not affect basal $[\text{Ca}^{2+}]_i$ (Fig. 4C).

To investigate whether removal of calmodulin binding from TRPV5 alters the Ca^{2+} sensitivity of the channel, the whole-cell patch clamp technique was used. The Ca^{2+} current generated by TRPV5-WT was evaluated by the application of a

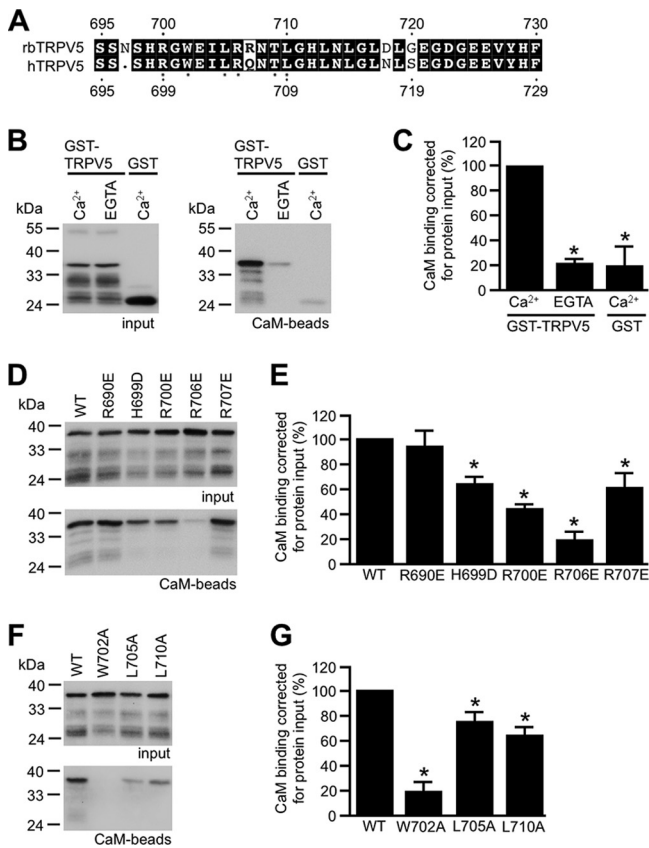


FIG. 3. Assay of GST-TRPV5 binding to calmodulin. (A) Sequence alignment of calmodulin binding domains in the last part of the TRPV5 C terminus for rabbit (rb) and human species. Note the difference in the numbering of the amino acid positions. The dots indicate the residues involved in the binding of calmodulin, as identified by NMR spectroscopy. (B) Typical blot of precipitation of GST and GST-TRPV5 (GST-V5) in the presence of 1 mM Ca²⁺ or 5 mM EGTA (only TRPV5-WT). Input, total bacterial cell lysate containing TRPV5; CaM-beads, TRPV5 precipitation by calmodulin beads. (C) Quantification of TRPV5-Ca²⁺ (*n* = 4), TRPV5-EGTA (*n* = 3), and GST-Ca²⁺ (*n* = 4) precipitation. The asterisk denotes a significant difference (*P* < 0.05) from TRPV5-Ca²⁺. (D and E) Representative blot and quantification of TRPV5-WT, -R690E, -H699D, -R700E, -R706E, and -R707E in the presence of 1 mM Ca²⁺ (all conditions, *n* = 3). (F and G) Representative blot and quantification of TRPV5-WT, -W702A, -L705A, and -L710A (all conditions, *n* = 4). *, *P* < 0.05 versus TRPV5-WT.

hyperpolarizing voltage step to -100 mV from a holding potential of +70 mV. This elicited a strong inward rectification, followed by rapid Ca²⁺-dependent inactivation, which is characteristic for the TRPV5 channel (Fig. 5A) (32). The mutant channels TRPV5-W702A and TRPV5-R706E exhibited significantly slower Ca²⁺-dependent channel inactivation than TRPV5-WT (Fig. 5A and B). Na⁺ current measurements in nominally divalent-free (DVF) solution (20 μM EDTA) demonstrated similar current/voltage profiles and current densities for both mutants and TRPV5-WT (Fig. 5C and D).

PTH-mediated TRPV5 stimulation is due to the release of calmodulin. PTH triggers a cyclic AMP (cAMP) pathway that induces protein kinase A (PKA) activation and subsequent phosphorylation of the T709 residue of TRPV5 resulting in channel stimulation (5). As residue T709 is located within the

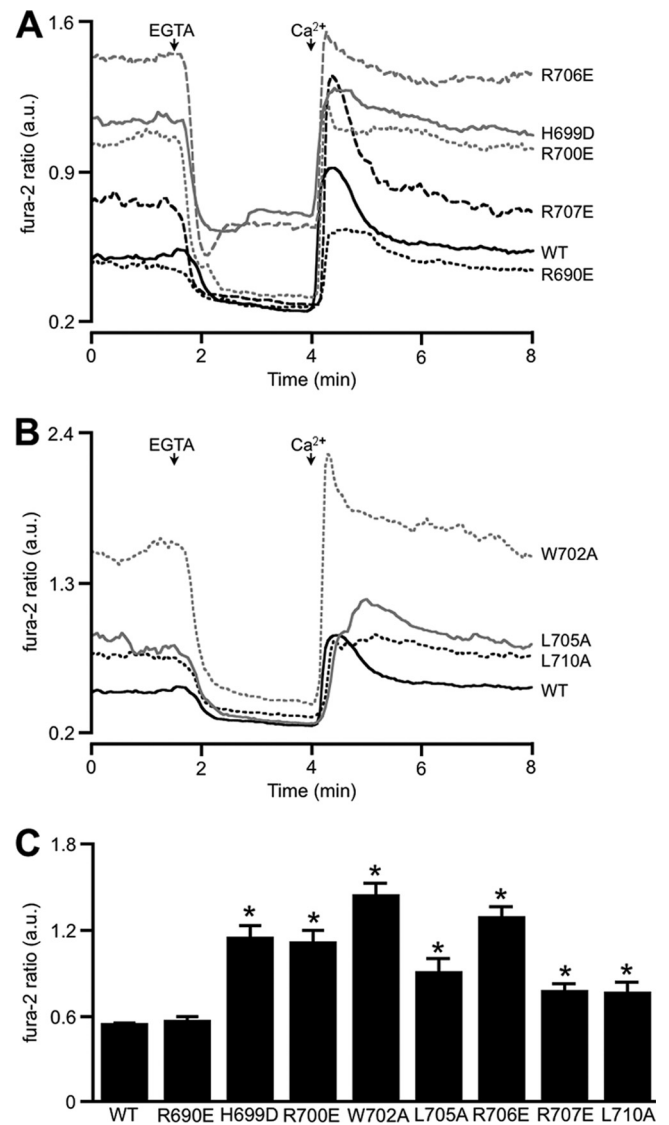


FIG. 4. Fura-2 analysis of TRPV5-WT and various point mutants. (A and B) Representative fura-2 traces in arbitrary units (a.u.) of HEK293 cells transiently transfected with TRPV5-WT and the different point mutants. At *t* = 1.5 min the extracellular Ca²⁺ solution (1.4 mM) was replaced by an EGTA solution (2 mM). At *t* = 4 min the EGTA solution was again replaced for Ca²⁺ (1.4 mM). (C) Averaged fura-2 levels of TRPV5-WT (*n* = 36) and TRPV5 mutants R690E (*n* = 25), H699D (*n* = 25), R700E (*n* = 29), W702A (*n* = 26), L705A (*n* = 25), R706E (*n* = 25), R707E (*n* = 46), and L710A (*n* = 40) at *t* = 0. *, *P* < 0.05 versus TRPV5-WT. Data from at least three independent experiments are shown.

calmodulin binding site, we hypothesized that phosphorylation of T709 might prevent calmodulin binding, resulting in increased TRPV5 activity. Therefore, the point mutation mimicking the phosphorylated state of TRPV5 (T709D) was introduced in GST-TRPV5 to study the effect on calmodulin binding. The calmodulin-Sepharose beads precipitated less of the T709D mutant than TRPV5-WT, whereas precipitation of the constitutively nonphosphorylated mutant T709A was similar to that of the WT (Fig. 6A and B). Next, the role of calmodulin in TRPV5 stimulation by PTH was studied in

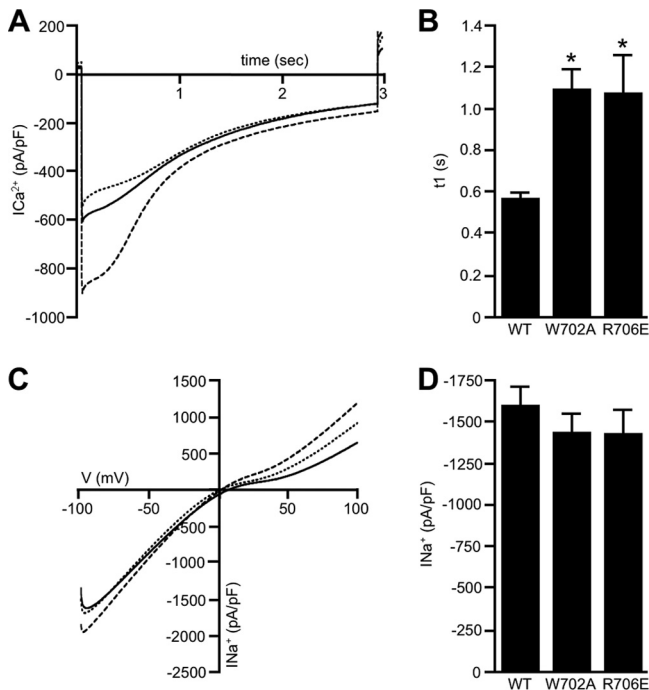


FIG. 5. TRPV5-W702A and TRPV5-R706E exhibit diminished Ca^{2+} -induced inactivation. (A) Averaged traces of inward Ca^{2+} currents measured with 10 mM extracellular Ca^{2+} during a 3-s step to -100 mV from a holding potential of $+70$ mV in HEK293 cells expressing either TRPV5-WT (dashed line), TRPV5-W702A (dotted line), or TRPV5-R706E (solid line). (B) Average t_1 (time after which channel activity is inhibited by 50%) values of TRPV5-WT ($n = 13$), TRPV5-W702A ($n = 10$), and TRPV5-R706E ($n = 8$) depicted in black bars analyzed via mono-exponential fitting. *, $P < 0.05$ versus TRPV5-WT. (C) I/V profiles of TRPV5-WT (dashed line), TRPV5-W702A (dotted line), or TRPV5-R706E (solid line). Cells were held at $+20$ mV, and voltage ramps of 450 ms ranging from -100 to $+100$ mV were applied to measure I/V relations. (D) Average Na^+ current density at -80 mV of TRPV5-WT ($n = 13$), TRPV5-W702A ($n = 10$), and TRPV5-R706E ($n = 8$).

living cells. To this end, we coexpressed the PTH receptor and TRPV5-WT or the TRPV5-W702A mutant, which has a disrupted calmodulin binding site, in HEK293 cells and assessed TRPV5 function by fura-2 analysis. PTH stimulation increased $[Ca^{2+}]_i$ of TRPV5-WT (Fig. 6C and D). The $[Ca^{2+}]_i$ in HEK293 cells expressing TRPV5-W702A or the negative control TRPV5-T709A did not change upon PTH stimulation (Fig. 6C and D), indicating that PTH-mediated phosphorylation of T709 results in loss of calmodulin binding and, therefore, an increase in intracellular Ca^{2+} -levels.

TRPV5-W702A displays an increased channel-open probability and is not sensitive to PTH stimulation. To study the interplay between PTH stimulation and calmodulin binding to the TRPV5 C terminus at a single-channel level, cell-attached patch clamp analysis was employed. Using HEK293 cells transiently expressing TRPV5-WT or TRPV5-W702A, the patch pipette was attached to the cell without disrupting the membrane, and TRPV5 channel current was recorded using Na^+ as a charge carrier. Virtually no channel activity was detected at positive membrane potentials for both TRPV5-WT (Fig. 7A) and TRPV5-W702A (Fig. 7B). A voltage step protocol from

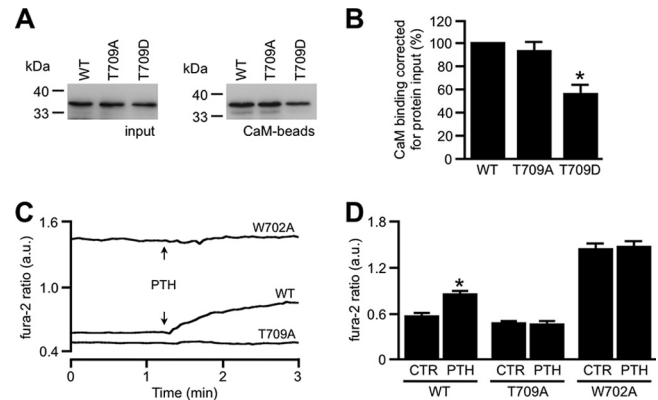


FIG. 6. Role of calmodulin in PTH stimulation of TRPV5. (A and B) Representative blot and quantification of GST-TRPV5 precipitation using calmodulin beads. (C) Fura-2 ratio in arbitrary units (a.u.) of HEK293 cells expressing TRPV5-WT ($n = 52$), -T709A ($n = 51$), and -W702A ($n = 36$) upon PTH stimulation (10 nM) at $t = 75$ s. (D) Statistical analysis of basal fura-2 ratio at $t = 0$ (control [CTR]) and after PTH stimulation at $t = 3$ min. *, $P < 0.05$ versus CTR. Data from at least three independent experiments are shown. CaM, beads.

-100 to 80 mV established a current/voltage (I/V) relationship revealing an average single-channel conductance of 64 ± 7 pS ($n = 4$) for TRPV5-WT and 69 ± 5 pS ($n = 3$) for TRPV5-W702A (Fig. 7C). After a stable recording of TRPV5 channel current at -80 mV was obtained, PTH was added to the bath solution. TRPV5 activity is illustrated by averaged data of channel-open probability (NP_o , where N is the number of channels and P_o is open probability of the channel) of 10-s intervals of multiple recordings. The average NP_o at basal conditions (min 0 to 1) of HEK293 cells expressing TRPV5-WT was significantly smaller than the NP_o of TRPV5-W702A (Fig. 7D). PTH significantly increased the NP_o of TRPV5-WT, while the NP_o of TRPV5-W702A was not affected by PTH treatment (Fig. 7D). To visualize the kinetics of channel activity upon PTH stimulation, the averaged NP_o levels of TRPV5-WT and -W702A are depicted in 10-s intervals in Fig. 7E and F, respectively. Maximal TRPV5 open probability is reached 1 min after PTH stimulation.

DISCUSSION

This study demonstrates the pivotal role of calmodulin in Ca^{2+} -dependent TRPV5 inactivation and the modulation of this mechanism by PTH. This conclusion is based on the following findings: (i) a calmodulin binding site is present in the last part of the TRPV5 C terminus; (ii) Ca^{2+} -dependent interaction with this part of the C terminus occurs in a mode enabling one molecule of calmodulin to bind two TRPV5 C termini; (iii) loss of calmodulin binding enhances TRPV5-mediated Ca^{2+} influx due to decreased Ca^{2+} -dependent inactivation; and (iv) PTH stimulation diminishes calmodulin binding to the C terminus, leading to an elevation of TRPV5 single-channel activity.

Using NMR spectroscopy, we demonstrated that the C-terminal part of TRPV5 contains a calmodulin binding motif, which allows two C-terminal peptides to bind one molecule of calmodulin in a Ca^{2+} -dependent manner. The following

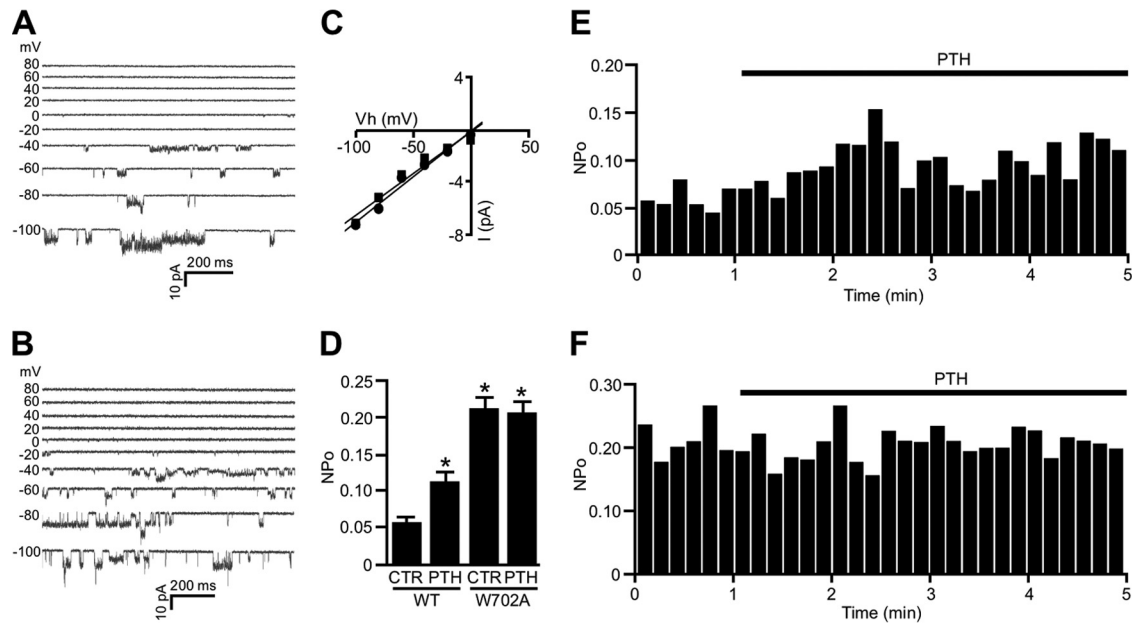


FIG. 7. PTH stimulates single-channel activity of TRPV5-WT but not V5-W702A. (A and B) Cell-attached single-channel recordings were made from HEK293 cells expressing TRPV5-WT or TRPV5-W702A. Channel activity was elicited by step potentials varying from -100 to 80 mV for TRPV5-WT (A) and TRPV5-W702A (B). (C) Amplitude histograms were constructed from regions of the single-channel recordings and were fitted by three Gaussian functions corresponding to closed, one open, or two open levels. The averaged calculated slope conductance was 64 ± 7 pS for TRPV5-WT ($n = 4$) and 69 ± 5 pS for TRPV5-W702A ($n = 3$). (D) The average NP_o upon PTH stimulation was assessed by averaging min 2 and 3 while the control (CTR) value reflects min 0 to 1. PTH significantly elevates NP_o in TRPV5-WT-expressing cells, whereas it does not influence NP_o in cells expressing TRPV5-W702A. Under control conditions the NP_o of TRPV5-W702A is significantly higher than that of TRPV5-WT. *, $P < 0.05$ versus TRPV5 CTR. (E and F) Averaged recording of TRPV5-WT (E, $n = 5$) and TRPV5-W702A (F, $n = 6$) over time using cell-attached patch clamp (holding potential, -80 mV). NP_o values were the average of 10-s intervals.

TRPV5 residues were suggested to be critical for this interaction: R699, W702, L705, R706, T709, and L710 (numeration for rabbit TRPV5). Stoichiometries different from 1:1 have previously been reported for calmodulin-protein interactions. For aquaporin-0 (AQP0), it was also shown that one calmodulin binds two C-terminal peptides, as well as two intact AQP0 molecules (28). The proposed structural model suggests that in the presence of Ca^{2+} , calmodulin binds the C termini from two neighboring AQP0 monomers, locking these domains in an orientation that seemingly blocks the pores of two AQP0 monomers within the tetramer. Another example originates from the crystal structure of cardiac L-type calcium channels (9). Here, calmodulin binding to the C-terminal regulatory domain results in two different complexes of calmodulin, one in a standard 1:1 binding mode and one in an extended conformation bridging two parts of the C termini together. Since TRPV5 is a tetramer in its functional state, calmodulin might bridge the C termini of the two monomers in a similar fashion. However, to decipher the gating mechanism by which Ca^{2+} -bound calmodulin modulates TRPV5 inactivation, more structural data are required.

Calmodulin plays an essential role in numerous Ca^{2+} -dependent processes. It is present in all eukaryotic cells and is highly conserved (100% in animals) (1). To further study the role of calmodulin in the Ca^{2+} -dependent inactivation of TRPV5, the C-terminal residues of the channel critical for interaction with calmodulin (as suggested by NMR spectroscopy) were mutated. Residues essential for calmodulin binding are also known to have positive and bulky hydrophobic side

chains (15, 36). Fura-2 analysis of these mutants demonstrated that loss of calmodulin binding elevated TRPV5-mediated Ca^{2+} influx, leading to an increased $[Ca^{2+}]_i$. TRPV5-W702A and -R706E mutants displayed the highest intracellular Ca^{2+} levels, which was in line with the nearly complete loss of calmodulin binding of these mutants. Next, patch clamp analysis was used in order to identify the molecular mechanism underlying TRPV5 activation upon release of calmodulin. Whole-cell Na^+ currents of mutants W702A and R706E were not different from those of TRPV5-WT, suggesting that WT and mutant channels have similar plasma membrane expression levels. Both the TRPV5-W702A and -R706E mutant exhibited a decreased peak Ca^{2+} current and a reduced Ca^{2+} -dependent inactivation in comparison to TRPV5-WT. A similar phenomenon was recently described for the helix-breaking mutation M490P, which almost completely abolished TRPV5 inactivation upon influx of 10 mM Ca^{2+} (18). This mutant displayed whole-cell Na^+ currents similar to those of TRPV5-WT, and the peak Ca^{2+} current was reduced, similar to results with the TRPV5 mutants W702A and R706E. It remains to be confirmed whether the mutation M490P in the channel pore and C-terminal mutations induce the same effects on TRPV5 channel function. It would therefore be interesting to study the potential interaction of the TRPV5 C terminus with the channel pore.

Finally, we demonstrated that loss of calmodulin binding results in an elevation of the TRPV5 open probability. This indicates that calmodulin in a Ca^{2+} -dependent manner reduces the time that the TRPV5 channel spends in an open

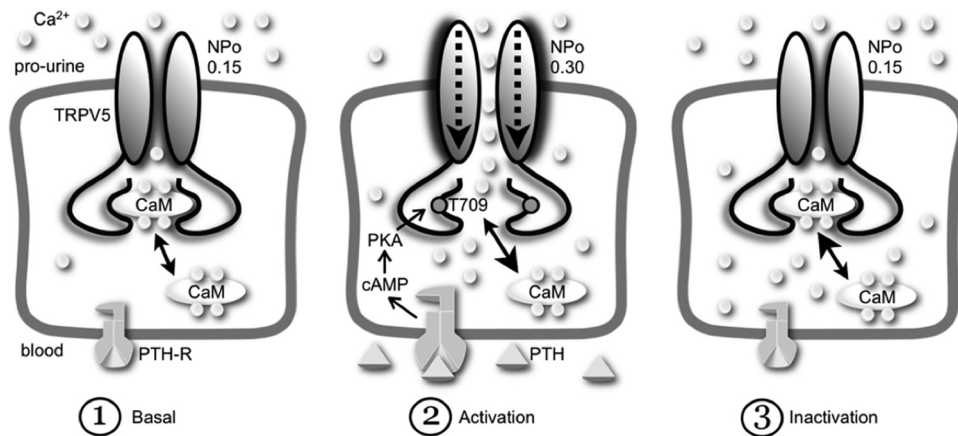


FIG. 8. Model illustrating TRPV5 stimulation by parathyroid hormone. Panel 1 illustrates TRPV5 regulation under basal conditions. Panel 2 displays TRPV5 regulation at low extracellular Ca^{2+} levels. PTH release in blood stimulates the PTH receptor, triggering a cAMP-PKA pathway. This results in the phosphorylation of the TRPV5 C terminus at residue T709. Phosphorylation of T709 diminishes calmodulin (CaM) binding at the last part of the C terminus, increasing channel-open probability and inducing an enlarged TRPV5-mediated Ca^{2+} influx into the cell. Panel 3 demonstrates the situation in which Ca^{2+} homeostasis is reached, and the increased intracellular Ca^{2+} levels inactivate TRPV5 activity, again via the binding of calmodulin. AC, adenylyl cyclase.

conformation. The role of calmodulin in single-channel regulation was studied by others previously (10, 29); however, the structural modulation of a channel by calmodulin is still unknown (4, 27). Thus, TRPV5 inactivation upon the influx of Ca^{2+} is mediated by calmodulin to prevent excessive Ca^{2+} influx, which is detrimental for the cell. Ca^{2+} -dependent channel inactivation by calmodulin was also demonstrated for several other members of the TRP family (for an overview, see reference 37) and voltage-gated Ca^{2+} channels (17, 26, 27). The indispensable role for calmodulin in TRPV5 regulation also becomes apparent by studying the alignment of the TRPV5/TRPV6 C termini of different mammalian, reptile, and fish species. The critical calmodulin-interacting residues W702 and R706 appear to be fully conserved (see Fig. S1 in the supplemental material).

Recently, PTH-mediated PKA activation was shown to induce TRPV5 stimulation via phosphorylation of the channel at residue T709, ultimately resulting in an elevation of the channel-open probability (5). As the T709 residue is located within the novel calmodulin binding site identified in this study, the role of T709 phosphorylation in calmodulin binding was studied using the constitutively active T709D mutant. This T709D mutant displayed a decrease in calmodulin binding compared to level of the WT channel or the constitutively inactive T709A mutant. Then, using living cells, the interplay between T709 phosphorylation and calmodulin binding in the regulation of TRPV5 function was examined. When PTH-induced phosphorylation of T709 releases calmodulin from the TRPV5 C terminus and thereby increases TRPV5-mediated Ca^{2+} influx, a TRPV5 mutant with a disrupted calmodulin binding site should not respond to PTH stimulation. To test this hypothesis we stimulated TRPV5-W702A with PTH as this mutant does not interact with calmodulin and still harbors an intact PKA phosphorylation site around T709. The R706E mutant was not used as the R706E mutation might affect phosphorylation of T709 according to the prediction server NetPhosk (www.cbs.dtu.dk/services). TRPV5-W702A did not respond to PTH

stimulation, as assessed by fura-2 and cell-attached patch clamp analysis, indicating that the PTH-mediated reduction of calmodulin binding is essential for TRPV5 activation. These results demonstrate that PKA-mediated phosphorylation of T709 diminishes calmodulin binding to the TRPV5 C terminus and, thereby, increases the activity of the channel. Moreover, PTH stimulation did not enhance the TRPV5 activity to a similar extent as introduction of the W702A mutation. This is in agreement with the more severe reduction in calmodulin binding of the W702A mutation in comparison to the T709D mutation.

The counteraction of channel phosphorylation on calmodulin binding is in line with *in vitro* studies of other ion channels (11, 19, 21, 28, 35). For the close homologue TRPV6, fluorescence resonance energy transfer experiments revealed a Ca^{2+} -dependent and dynamic interaction of calmodulin with the last part of the TRPV6 C terminus (8). Another study showed that phosphorylation of a PKC consensus site located within a C-terminal calmodulin binding domain in hTRPV6 diminished calmodulin binding to this domain. This, however, was demonstrated only *in vitro* and does not apply to rabbit or mouse TRPV6 (21). In the present study, we implemented a physiological stimulus on living cells and thereby established an interplay between PTH-mediated phosphorylation at the fully conserved residue T709 and calmodulin binding, demonstrating an essential role for calmodulin in TRPV5 stimulation by PTH.

PTH is released from the parathyroid gland upon low blood Ca^{2+} levels and acts on the distal part of the nephron to stimulate active Ca^{2+} reabsorption in order to restore Ca^{2+} homeostasis. Here, we demonstrated that PTH induced PKA-mediated phosphorylation of residue T709 of the TRPV5 channel, thereby diminishing the binding of calmodulin to the channel C terminus. Calmodulin release from the C terminus increased the channel-open probability, eventually stimulating TRPV5-mediated Ca^{2+} influx (Fig. 8).

ACKNOWLEDGMENTS

This work was financially supported in part by grants from the Dutch Kidney Foundation (C03.6017 and C06.2170) and the Netherlands Organization for Scientific Research (NWO-ALW 814.02.001, NWO-CW 700.55.302, 700.55.443, and 700.57.101, and ZonMw 9120.6110). Lead Pharma Holding B.V. is kindly acknowledged for financial support to Marco Felici. J.G.J.H. is supported by an EURYI award.

We thank C. Klee for the calmodulin plasmid and AR58 cells, N. M. Link for providing the pGEV2 vector, and Nicolien Beld for technical assistance.

REFERENCES

- Balshaw, D. M., N. Yamaguchi, and G. Meissner. 2002. Modulation of intracellular calcium-release channels by calmodulin. *J. Membr. Biol.* **185**:1–8.
- Bertini, I., et al. 2009. Accurate solution structures of proteins from X-ray data and a minimal set of NMR data: calmodulin-peptide complexes as examples. *J. Am. Chem. Soc.* **131**:5134–5144.
- Bodenhausen, G. R., J. David. 1980. Natural abundance nitrogen-15 NMR by enhanced heteronuclear spectroscopy. *Chem. Phys. Lett.* **69**:185–189.
- Cui, J. 2010. Reduction of CaV channel activities by Ca²⁺-CaM: inactivation or deactivation? *J. Gen. Physiol.* **135**:297–301.
- de Groot, T., et al. 2009. Parathyroid hormone activates TRPV5 via PKA-dependent phosphorylation. *J. Am. Soc. Nephrol.* **20**:1693–1704.
- de Groot, T., S. Verkaart, Q. Xi, R. J. Bindels, and J. G. Hoenderop. 2010. The identification of histidine-712 as a critical residue for constitutive TRPV5 internalization. *J. Biol. Chem.* **285**:28481–28487.
- Delaglio, F., et al. 1995. NMRPipe: a multidimensional spectral processing system based on UNIX pipes. *J. Biomol. NMR* **6**:277–293.
- Derler, I., et al. 2006. Dynamic but not constitutive association of calmodulin with rat TRPV6 channels enables fine tuning of Ca²⁺-dependent inactivation. *J. Physiol.* **577**:31–44.
- Fallon, J. L., et al. 2009. Crystal structure of dimeric cardiac L-type calcium channel regulatory domains bridged by Ca²⁺* calmodulins. *Proc. Natl. Acad. Sci. U. S. A.* **106**:5135–5140.
- Fuentes, O., C. Valdivia, D. Vaughan, R. Coronado, and H. H. Valdivia. 1994. Calcium-dependent block of ryanodine receptor channel of swine skeletal muscle by direct binding of calmodulin. *Cell Calcium* **15**:305–316.
- Hisatsune, C., et al. 1997. Phosphorylation-dependent regulation of N-methyl-D-aspartate receptors by calmodulin. *J. Biol. Chem.* **272**:20805–20810.
- Hoenderop, J. G., B. Nilius, and R. J. Bindels. 2002. Molecular mechanism of active Ca²⁺ reabsorption in the distal nephron. *Annu. Rev. Physiol.* **64**:529–549.
- Hoenderop, J. G., et al. 2003. Renal Ca²⁺ wasting, hyperabsorption, and reduced bone thickness in mice lacking TRPV5. *J. Clin. Invest.* **112**:1906–1914.
- Huth, J. R., et al. 1997. Design of an expression system for detecting folded protein domains and mapping macromolecular interactions by NMR. *Protein Sci.* **6**:2359–2364.
- James, P., T. Vorherr, and E. Carafoli. 1995. Calmodulin-binding domains: just two faced or multi-faceted? *Trends Biochem. Sci.* **20**:38–42.
- Lambers, T. T., A. F. Weidema, B. Nilius, J. G. Hoenderop, and R. J. Bindels. 2004. Regulation of the mouse epithelial Ca²⁺ channel TRPV6 by the Ca²⁺-sensor calmodulin. *J. Biol. Chem.* **279**:28855–28861.
- Lee, A., et al. 1999. Ca²⁺/calmodulin binds to and modulates P/Q-type calcium channels. *Nature* **399**:155–159.
- Lee, K. P., et al. 2010. A helix-breaking mutation in the epithelial Ca²⁺ channel TRPV5 leads to reduced Ca²⁺-dependent inactivation. *Cell Calcium* **48**:275–287.
- Minakami, R., N. Jinnai, and H. Sugiyama. 1997. Phosphorylation and calmodulin binding of the metabotropic glutamate receptor subtype 5 (mGluR5) are antagonistic in vitro. *J. Biol. Chem.* **272**:20291–20298.
- Montell, C. 2003. The venerable invertebrate invertebrate TRP channels. *Cell Calcium* **33**:409–417.
- Niemeyer, B. A., C. Bergs, U. Wissenbach, V. Flockerzi, and C. Trost. 2001. Competitive regulation of CaT-like-mediated Ca²⁺ entry by protein kinase C and calmodulin. *Proc. Natl. Acad. Sci. U. S. A.* **98**:3600–3605.
- Nilius, B., et al. 2001. Modulation of the epithelial calcium channel, ECaC, by intracellular Ca²⁺. *Cell Calcium* **29**:417–428.
- Nilius, B., et al. 2000. Whole-cell and single channel monovalent cation currents through the novel rabbit epithelial Ca²⁺ channel ECaC. *J. Physiol.* **527**:239–248.
- Nilius, B., et al. 2001. The single pore residue Asp542 determines Ca²⁺ permeation and Mg²⁺ block of the epithelial Ca²⁺ channel. *J. Biol. Chem.* **276**:1020–1025.
- Nilius, B., et al. 2003. The carboxyl terminus of the epithelial Ca²⁺ channel ECaC1 is involved in Ca²⁺-dependent inactivation. *Pflugers Arch.* **445**:584–588.
- Peterson, B. Z., C. D. DeMaria, J. P. Adelman, and D. T. Yue. 1999. Calmodulin is the Ca²⁺ sensor for Ca²⁺-dependent inactivation of L-type calcium channels. *Neuron* **22**:549–558.
- Qin, N., R. Olcese, M. Bransby, T. Lin, and L. Birnbaumer. 1999. Ca²⁺-induced inhibition of the cardiac Ca²⁺ channel depends on calmodulin. *Proc. Natl. Acad. Sci. U. S. A.* **96**:2435–2438.
- Reichow, S. L., and T. Gonen. 2008. Noncanonical binding of calmodulin to aquaporin-0: implications for channel regulation. *Structure* **16**:1389–1398.
- Rycroft, B. K., and A. J. Gibb. 2002. Direct effects of calmodulin on NMDA receptor single-channel gating in rat hippocampal granule cells. *J. Neurosci.* **22**:8860–8868.
- van de Graaf, S. F., R. J. Bindels, and J. G. Hoenderop. 2007. Physiology of epithelial Ca²⁺ and Mg²⁺ transport. *Rev. Physiol. Biochem. Pharmacol.* **158**:77–160.
- van de Graaf, S. F., et al. 2003. Functional expression of the epithelial Ca²⁺ channels (TRPV5 and TRPV6) requires association of the S100A10-annexin 2 complex. *EMBO J.* **22**:1478–1487.
- Vennekens, R., et al. 2000. Permeation and gating properties of the novel epithelial Ca²⁺ channel. *J. Biol. Chem.* **275**:3963–3969.
- Vennekens, R., et al. 2001. Pore properties and ionic block of the rabbit epithelial calcium channel expressed in HEK 293 cells. *J. Physiol.* **530**:183–191.
- Vranken, W. F., et al. 2005. The CCPN data model for NMR spectroscopy: development of a software pipeline. *Proteins* **59**:687–696.
- Warr, C. G., and L. E. Kelly. 1996. Identification and characterization of two distinct calmodulin-binding sites in the Trp1 ion-channel protein of *Drosophila melanogaster*. *Biochem. J.* **314**:497–503.
- Yap, K. L., et al. 2000. Calmodulin target database. *J. Struct. Funct. Genomics* **1**:8–14.
- Zhu, M. X. 2005. Multiple roles of calmodulin and other Ca²⁺-binding proteins in the functional regulation of TRP channels. *Pflugers Arch.* **451**:105–115.